

Emerging microengineered tools for functional analysis and phenotyping of blood cells

Xiang Li^{1,2}, Weiqiang Chen^{1,2}, Zida Li^{1,2}, Ling Li³, Hongchen Gu⁴, and Jianping Fu^{1,2,5}

¹ Integrated Biosystems and Biomechanics Laboratory, University of Michigan, Ann Arbor, MI 48109, USA

² Department of Mechanical Engineering, University of Michigan, Ann Arbor, MI 48109, USA

³ Department of Precision Instruments, Tsinghua University, Beijing 100084, China

⁴ School of Biomedical Engineering, Shanghai Jiao Tong University, Shanghai 200030, China

⁵ Department of Biomedical Engineering, University of Michigan, Ann Arbor, MI 48109, USA

The available techniques for assessing blood cell functions are limited considering the various types of blood cell and their diverse functions. In the past decade, rapid advances in microengineering have enabled an array of blood cell functional measurements that are difficult or impossible to achieve using conventional bulk platforms. Such miniaturized blood cell assay platforms also provide the attractive capabilities of reducing chemical consumption, cost, and assay time, as well as exciting opportunities for device integration, automation, and assay standardization. This review summarizes these contemporary microengineered tools and discusses their promising potential for constructing accurate *in vitro* models and rapid clinical diagnosis using minimal amounts of whole-blood samples.

Microengineered tools for functional blood cell analysis

Human blood circulating in the body reaches and exchanges information with every tissue through the vascular network and is therefore an important indicator of the functional status of the human body. Many life-threatening diseases either are directly caused by abnormalities of the blood or blood flow (e.g., ischemic heart disease, stroke, diabetes) or can be detected through careful examination of molecular and cellular biomarkers circulating in the blood (e.g., cancer, HIV/AIDS, tuberculosis) [1–4]. Because of their ready availability, blood cell analysis and phenotyping are arguably the most common and important tests used in the clinic to provide physiological or pathological information for disease diagnosis and staging, treatment selection, safety and efficacy monitoring, and drug-dose adjustment.

Complementary to complete blood count and morphological analysis, functional blood cell analysis is sometimes necessary as it provides direct information regarding the functional status of the human body. Red blood cell (RBC)

fragility and deformability [5], white blood cell (WBC) immune response [6], and platelet aggregation [7] are among the most common functional tests performed on blood cells. However, the available techniques for assessing blood cell functions are limited, especially when considering the various types of blood cell and their diverse functions involved in different physiological and pathological contexts. Moreover, conventional tools for analyzing blood cell functions are bulky and costly, rely on complex manual operations and sample preparation, and are designed exclusively for research or clinical settings [8,9]. Due to these common technical limitations, traditional blood cell functional analysis and phenotyping tools remain difficult to standardize and do not meet the needs of modern clinical and health-care applications, including accurate and rapid testing of the diverse functions of blood cells, point-of-care diagnostics, and the construction of highly reliable *in vitro* models [10].

Recent advances in microengineering have offered researchers and clinicians an exciting new set of tools for accurate, fast, and affordable analysis of the cellular components of the blood (Box 1) [11,12]. The ability to precisely control and manipulate single cells in a defined environment has enabled an array of functional measurements that are difficult or impossible to achieve on conventional bulk platforms. Such miniaturized assays also provide the attractive capabilities of reducing chemical consumption, cost, and assay time, as well as exciting opportunities for integrating blood cell analysis with upstream blood sample preparation on a monolithic platform [13]. This review introduces recent achievements in microengineered tools for the functional analysis and phenotyping of blood cells. Examples of how microengineered tools are adapted for analysis of RBCs, WBCs, and platelets are discussed. Finally, we offer speculations on the research directions and potential opportunities for microengineered blood cell analysis tools to meet current and future challenges of clinical and laboratory diagnosis.

Functional analysis of RBCs

RBCs are the most abundant cells in human blood, with a normal concentration of around 5×10^9 cells/ml. With a

Corresponding author: Fu, J. (jpfu@umich.edu).

Keywords: blood cell; functional analysis; phenotyping; microengineering; microfluidics.

0167-7799/

© 2014 Elsevier Ltd. All rights reserved. <http://dx.doi.org/10.1016/j.tibtech.2014.09.003>

Box 1. The microengineered toolbox

Laminar flow

Fluid flow in most microfluidic devices is laminar due to the small geometrical size of the devices. The stable and predictable flow field for laminar flow makes it easy to maintain a predefined shear rate, the magnitude of which can be tuned by adjusting flow rate or microchannel geometry. Laminar flow can also be manipulated to create complex flow patterns such as flow focusing [28,87] and hydrodynamic stretching [25,58] (Figure 1A).

Constriction channels

Microfluidic constriction channels are microchannels whose width is smaller than that of cells passing through the channels (Figure 1B). They have been extensively used as mechanical means to deform blood cells to assess their deformability. For ease of fabrication, almost all constriction microchannels have a rectangular cross-section, which differs from the circular blood-vessel shape. Despite this difference, constriction microchannels have been successful in retaining *in vivo* blood cell functionalities [88].

Microwell array

Microwell array is used for isolation and analysis of single blood cells (Figure 1C) [89]. To ensure single-cell trapping, a blood cell suspension with a proper cell density is placed onto the microwell array and allowed to sediment into the microwells. One microwell

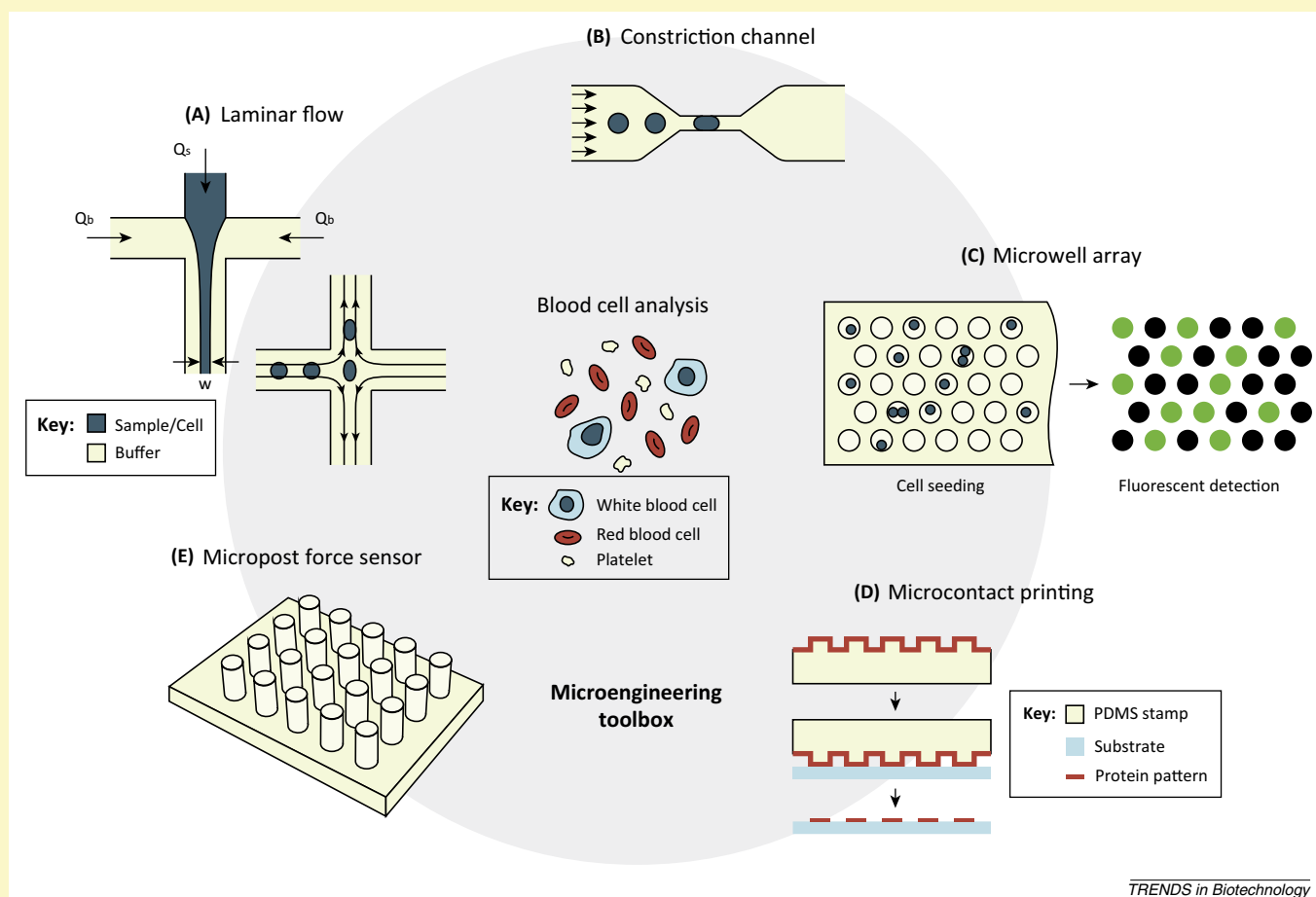
array thus contains up to thousands of single cells, with each single cell trapped in an individual microwell. Each of the microwells creates a confined cellular environment that can effectively concentrate analytes and amplify detection sensitivity.

Microcontact printing

Microcontact printing (μ CP) is a simple yet highly versatile method to pattern proteins on various kinds of substrate [90,91]. Briefly, a monolayer of protein is coated on a micropatterned elastomeric stamp. The stamp is then brought into direct contact with the target substrate, to which proteins can preferentially bind. Only proteins in direct contact with the substrate are transferred onto it (Figure 1D). For blood cell functional analysis, μ CP is mainly used for patterning adhesion proteins for cell adhesion and aggregation.

Micropost force sensor

The micropost force sensor was originally developed to measure cell traction force (Figure 1E). It contains a regular array of vertical elastomeric posts with a post diameter down to 1–2 μ m. The tips of the microposts are functionalized with adhesive proteins, with the post sidewalls passivated with nonadhesive molecules to ensure that cells adhere to the post tops. When a cell exerts lateral contractile force on the underlying posts, the posts will bend and the magnitude of the cell contractile forces can be inferred by the displacements of the post tips.



TRENDS in Biotechnology

Figure 1. The microengineered toolbox. **(A)** Microfluidic control of laminar flow. In one example, sample flow is focused by buffer flows to width w , which is determined by the ratio of buffer flow rate (Q_b) to sample flow rate (Q_s). In another example, extensional shear force was generated at the intersection of four perpendicular flows. **(B)** Microfluidic constriction channel for cell deformation assays. **(C)** Microwell array for simultaneous capture and analysis of thousands of single cells. Fluorescence-based biodetection [e.g., enzyme-linked immunosorbent assay (ELISA)] can be used to measure the amount of protein secreted by each single cell trapped in the microwell. **(D)** Microcontact printing for selective surface functionalization. The protein is adsorbed on the micropatterned surface of a polydimethylsiloxane (PDMS) stamp before being transferred onto a substrate by direct contact of the two surfaces. **(E)** Micropost force sensor for measuring the contractile force of platelets and blood clots.

biconcave discoid shape and a diameter of 6–8 μm , they are highly differentiated cells that lack a nucleus and most organelles [5]. Two properties of RBCs – deformability and ATP release – are commonly measured for the clinical and laboratory diagnosis of diseases such as malaria, sickle-cell disease, and pulmonary hypertension [14–16].

Deformability of RBCs

Healthy RBCs are smooth and extremely deformable so that they can easily pass through the spleen and microcapillaries. Abnormal stiffness of RBCs is usually an indicator of disease. For example, in *Plasmodium falciparum*-infected malaria patients, RBCs gradually lose their deformability with progression of the infection and late-stage infected RBCs can become stiffer by a factor of 50 [14]. There is also loss of RBC deformability due to abnormal polymerization of hemoglobin in patients with sickle-cell disease [15]. In both diseases, hardened RBCs can impair blood circulation and may eventually lead to occlusion.

Conventional RBC deformability assays can be classified into bulk assays that measure the average effect on a RBC population and single-cell assays that assess the deformability of single RBCs [5]. In a commonly used filtration assay, anticoagulated blood flows through a filtration membrane with a pore diameter of 5 μm and the pressure drop across the membrane, which correlates with RBC deformability, is measured [17]. Because bulk RBC deformability assays deal with a RBC population, they cannot identify subsets of RBCs or rare RBCs that have direct pathological implications [18]. By contrast, single-cell deformability measurements such as micropipette aspiration [19] and ektacytometry [20] apply hydrostatic or shear force to individual RBCs while simultaneously monitoring their morphological changes using microscopy. However, due to the complexity of the experimental set-up and cumbersome assay procedures, single-cell assays for RBC deformability measurements tend to have a low throughput (1–10 cells/h).

The recent trend of using high-throughput and multiplex microfluidic technologies to redesign traditional bulk and single-cell deformability assays has significantly improved their performance. For instance, a microchannel network was constructed with a constant channel depth of 6 μm and varying channel widths of 6–70 μm (Figure 1A) [21]. An RBC suspension with a hematocrit of 40% was perfused through the network under a constant hydraulic pressure and the average RBC transit velocity was measured to indicate cell deformability. Compared with the conventional filtration assay, which works only under 1% hematocrit, this microfluidic perfusion assay was shown to be more sensitive to small changes of RBC deformability.

Microfluidic constriction channels that resemble micropipettes have also been developed for measuring the deformability of single RBCs in a high-throughput manner (Figure 1B) [22]. A 2D microfluidic constriction array, for example, is capable of measuring the deformability of 10^4 cells simultaneously [22,23]. Such high-throughput single-cell measurements made it possible to identify a small subset of *P. falciparum*-infected RBCs from a large background population of normal RBCs. Another strategy for

increasing single-cell assay throughput has been developed by continuously pushing single RBCs through a constriction while measuring the cell transition time in real time using integrated electrodes based on the Coulter principle [24]. A throughput of 10 cells/s was reported using such a continuous-flow operation.

The aforementioned microfluidic devices all utilize defined microscale constrictions to mechanically deform RBCs while the cells are passing through constrictions under the influence of external forces. However, such confined microfluidic environments unavoidably lead to clogging. A newly developed hydrodynamic stretching device can effectively avoid clogging by using inertia focusing and fluid shear force to stretch single RBCs [25]. The shape of the deformed RBCs was recorded using a high-speed camera and a cell-shape-elongation index was used to describe RBC deformability (Figure 1C).

Label-free cellular biomarkers such as mechanical deformability are attractive targets for point-of-care testing, as measuring such markers may eliminate the use of chemicals that are often costly and difficult to transport and store. With the ability for rapid, high-throughput measurements of the mechanical properties of RBCs, microfluidic deformability assays may provide promising solutions for rapid diagnostic testing for diseases such as malaria. It should be noted, however, that such microfluidic deformability assay platforms need more careful characterization and validation using clinical blood samples to fully assess their sensitivity, accuracy, and clinical utility.

ATP release by RBCs

RBC-derived ATP stimulates nitric oxide (NO) synthesis by endothelial cells, which in turn induces relaxation of vascular smooth muscle cells in the blood vessel wall to facilitate the passage of RBCs in narrow vascular regions [26,27]. Impaired ATP release has been shown to correlate with pulmonary hypertension [16]. ATP concentration is commonly measured using luciferase assays, which can be conveniently combined with a microfluidic constriction channel or flow focusing that deforms RBCs and triggers their ATP release (Figure 1D) [28]. An important advantage of such microfluidic ATP-releasing assays is the real-time detection capability, which is useful for providing biological insights into ATP biosynthesis. This feature was exploited in an elegant study investigating the time delay between cell deformation and ATP release in RBCs [29]. The microchannels used in this study contained a segment of narrow constriction to locally deform and stimulate single RBCs. Deformed RBCs were allowed to recover downstream of the narrow constriction. Using this device, it was shown that the response time between RBC deformation and ATP release was tens of milliseconds, and this delay decreased with increasing shear stress and was independent of RBC stiffness.

Functional analysis of WBCs

WBCs are functional units of the immune system that protects the human body from foreign invaders. The numbers, composition, and functional responses of WBCs change drastically in the presence of infections, malignancies, and autoimmune disorders. In particular, WBCs can

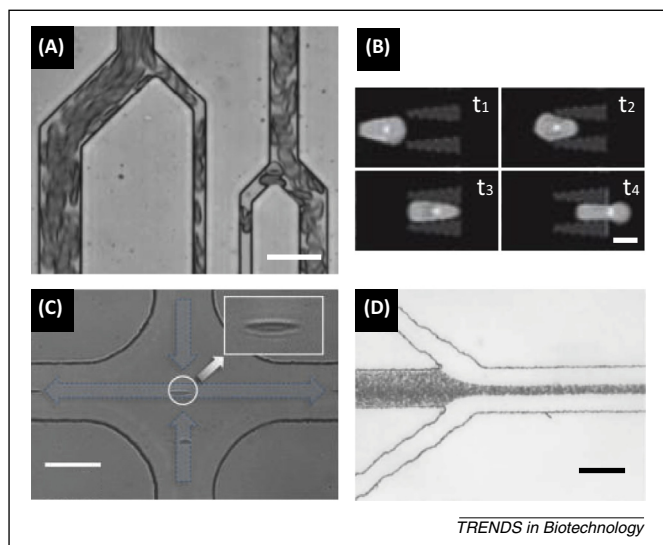


Figure 1. Microfluidic cell deformability assays for red blood cells (RBCs). (A) A microfluidic vasculature network to perfuse a RBC suspension, where RBCs were deformed by constriction channels [21]. Bar, 30 μm . Reproduced, with permission, from [21]. (B) Time-lapse images showing deformation of a single RBC moving through a constriction [22]. Bar, 5 μm . Reproduced, with permission, from [22]. (C) In a hydrodynamic stretching device using viscoelastic fluid, single RBCs were spontaneously focused to the center of the channel and stretched by shear force as they approached the intersection [25]. Bar, 50 μm . Reproduced, with permission, from [25]. (D) Flow focusing was used to deform RBCs and trigger their ATP release [28]. Bar, 100 μm . Reproduced, with permission, from [28].

secrete soluble proteins, termed ‘cytokines’, to regulate the growth, maturation, and responsiveness of immune cells. The production of interferon gamma (IFN- γ) by T cells, for example, correlates with the body’s ability to mount a vigorous immune response against tuberculosis infection [30]. Thus, detection of cytokine secretion from WBCs is of great importance both for fundamental understanding of human immunity and for immune monitoring in healthy humans and in those with allergy, asthma, autoimmunity, acquired or primary immunodeficiency, transplantation, or infection. In inflammatory response, WBCs also need to emigrate from the blood vessel to enter targeted tissues, a process dependent on WBC deformability and adhesion and the shear rate of the blood flow [31]. Here we focus on two types of WBC functional analysis – functional immunophenotyping and deformability measurements – that have recently been achieved using innovative microengineered tools.

Functional immunophenotyping of WBCs

Functional immunophenotyping refers to the identification of cytokine secretion levels by immune cells and can be conducted at the whole-cell population, subpopulation, or single-cell level [32]. Recently, various novel microengineered tools have been developed to improve traditional functional immunophenotyping assays for WBCs.

Miniaturized enzyme-linked immunosorbent assay/spot (ELISA/ELISpot)/AlphaLISA. ELISA/ELISpot is the current gold standard in quantifying cytokine secretion from WBCs. However, conventional ELISA/ELISpot requires multiple washings and incubations and is notorious for its tedious manual operation and prolonged assay time. Miniaturized ELISA/ELISpot was developed with the aim

of reducing sample consumption and assay time while maintaining high sensitivity [33–35]. Notably, miniaturized immunoassays are convenient for integration with upstream blood cell separation, and such integrated cell isolation and biodetection microfluidic devices are ideal for assessing the functional status of subsets of immune cells or even single immune cells. For example, microscale anti-CD4 and anti-CD8 antibodies were printed on polyethylene glycol (PEG) hydrogel-coated glass slides to capture CD4⁺ and CD8⁺ T cells directly from RBC-depleted blood samples (Figure 2A,B) [36]. On the same slide, next to anti-CD4 and anti-CD8 antibody spots, interleukin-2 (IL-2)- and IFN- γ -specific antibodies were printed to detect IL-2 and IFN- γ secreted from captured T cells, respectively [36]. This antibody array device was later successfully combined with a holographic imaging system for point-of-care applications [37].

Cellular heterogeneity is common in an isogenic cell population. Thus, quantitative immunophenotyping of single immune cells is desirable for the precise assessment of patient immune status [38,39]. By reducing the size of antibody spots on PEG gels, single immune cells were captured and cytokine secretions from the captured single cells were measured [40]. Another elegant technique for single-cell immunophenotyping is the microwell array designed for trapping individual WBCs in a confined microwell environment [41–43]. Cytokines secreted by single WBCs were confined in the microwell, resulting in significantly increased cytokine concentrations that were readily detected by antibodies coated on the coverslip sealing the microwell. This microwell immunophenotyping assay was successfully utilized for simultaneous quantification of three different cytokines secreted from single WBCs. More recently, the microwell array was combined with a high-density antibody barcode array for simultaneous detection of 14 cytokines secreted from single WBCs (Figure 2D) [44,45].

AlphaLISA is a newly developed, homogeneous, no-wash, bead-based chemiluminescence immunodetection assay [46]. Using AlphaLISA, a microfluidic immunophenotyping assay (MIPA) device capable of on-chip cell trapping, endotoxin stimulation, and *in situ* cytokine measurement was recently developed [47]. The MIPA device incorporated a polydimethylsiloxane (PDMS) micro-filtration membrane (PMM) for isolation and enrichment of WBCs. The PMM further allowed diffusion of cytokines secreted from WBCs trapped on the PMM to an underlying immunoassay chamber, where biodetection using AlphaLISA was conducted. The MIPA device required 20-fold fewer cells than traditional immunoassays and the total assay time was seven times shorter than conventional ELISA. More recently, the MIPA device was combined with antibody-coated microbeads for the isolation and immunophenotyping of different subpopulations of WBCs from whole-blood specimens (Figure 2C) [48].

Although all of the aforementioned methods used on-chip microwell or microfiltration structures to capture target immune cells, they still require some human intervention to conduct immunosensing. To address this limitation, a microfluidic system incorporating integrated microvalves was recently developed for single-cell isolation

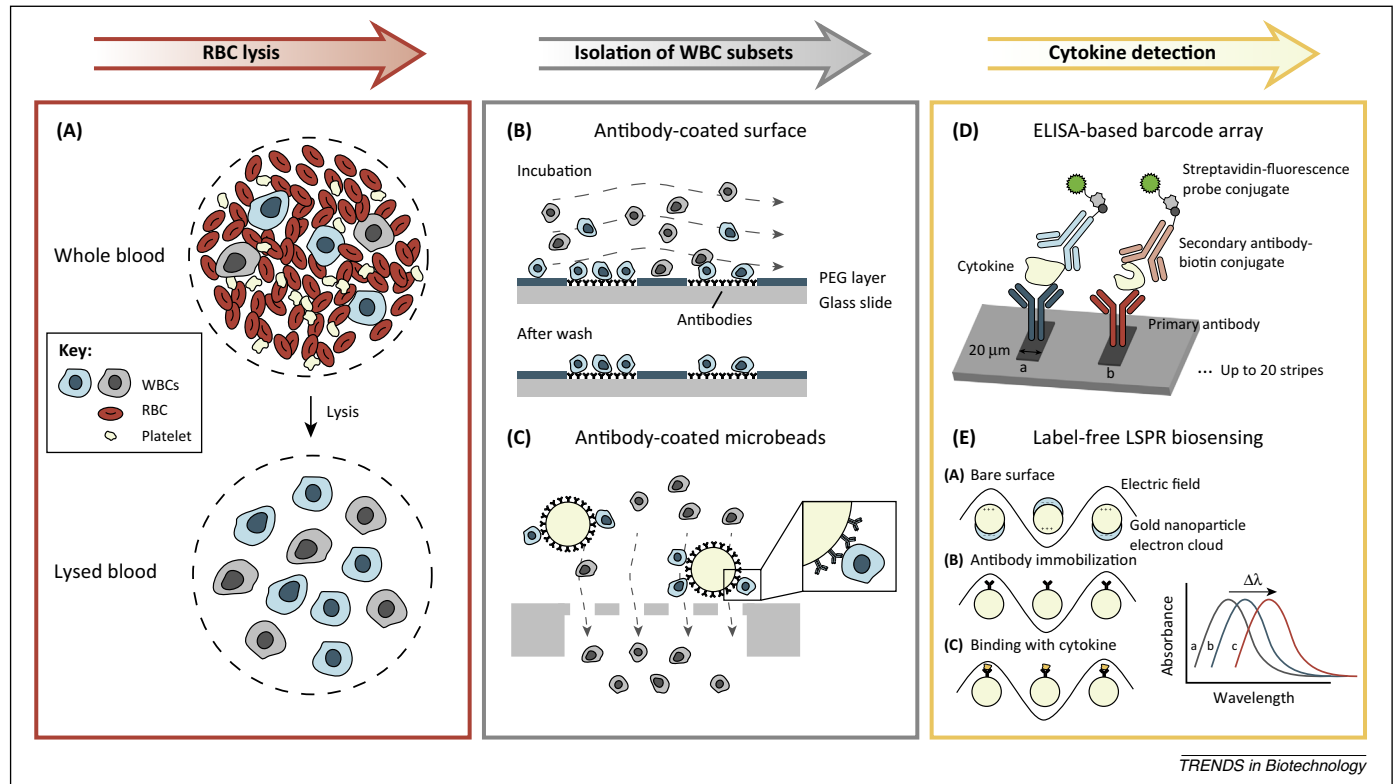


Figure 2. Paradigm of functional immunophenotyping of white blood cells (WBCs) using microengineered tools. Background red blood cells (RBCs) are first removed from whole-blood samples by lysis. Target WBC subsets are then isolated for cytokine secretion measurements. (A) Schematic of RBC lysis. (B) Antibody-coated surface for capturing subsets of WBCs. Target WBCs are bound to the antibodies coated on the glass slide during incubation while unbound cells are washed away [36]. (C) Isolation of subsets of WBCs using antibody-coated microbeads and microfilters. Target WBCs are retained on the filter as the microbead is larger than the filter pore size, while all other undesired WBCs pass through the filter freely [48]. (D) High-density antibody barcode using sandwich enzyme-linked immunosorbent assay (ELISA) for multiplexed detection of secreted proteins [44,45]. Adapted, with permission, from [44]. (E) Principle of localized surface plasmon resonance (LSPR) biosensing on a gold nanoparticle surface. The absorbance spectrum peak shift is used to quantify the amount of cytokine secreted by WBCs [51]. Adapted, with permission, from [51].

and automation of ELISA [49]. This highly integrated and automated system minimized human intervention and could potentially be utilized to improve the standardization of ELISA-based immunoassays.

Label-free methods. Conventional immunoassays require the labeling of analytes with fluorescent molecules for detection, rendering such immunoassays as end point-detection methods. To investigate dynamic immune responses, semiconductor nanowires were fabricated to enable label-free detection of low concentrations of antibodies and were further applied to the real-time monitoring of immune responses by WBCs [50]. More recently, a label-free immunoassay based on localized surface plasmon resonance (LSPR) was developed to detect tumor necrosis factor alpha (TNF- α) secreted by CD45⁺ cells isolated directly from human blood (Figure 2E) [51]. The assay time of these label-free immunosensing methods is much shorter than that of conventional ELISA; however, their clinical utility remains limited due to the manual sample preparation necessary before immunosensing [52]. Further optimization and integration of such label-free immunosensing methods with on-chip sample-preparation components would be required for these label-free methods to fulfill their potential for clinical applications [53].

Deformability of WBCs

Abnormality of WBC deformability is an important indicator of diseases such as sepsis [54] and diabetes

[55]. However, the low throughput associated with traditional deformability assays hampers their use in clinical applications. An on-chip micropipette aspiration system was developed to improve the throughput of traditional micropipette aspiration, where single WBCs were trapped and deformed at a constriction by a carefully designed microfluidic circuit [56]. The threshold pressure allowing the cell to pass through the microscale constriction was recorded. Using this device the authors were able to conduct single-cell deformability assays at a throughput of 30 cells/h. An astonishingly high throughput of 2000 cell/s was achieved by the deformability cytometer based on inertial focusing and fluidic shear force for cell deformation [57,58]. Interestingly, scatter plots of cell size and deformability (here defined as the ratio of the long-axis length of the cell body to its short-axis length) for a population of WBCs resembled cytometry plots, suggesting that cell size and deformability are completely decoupled traits for WBCs.

Functional analysis of platelets

Platelets are the smallest and second most abundant corpuscle in the blood. Platelets are derived from fragments of the cytoplasm of megakaryocytes and thus do not contain a nucleus. Normal platelets are discoid-shaped cells with a diameter of 2–4 μm and a thickness of about 0.5 μm . On activation, platelets change into a more rounded shape with long dendritic extensions to facilitate adhesion [59]. The primary functions of platelets are hemostasis and thrombosis, both of which are related to

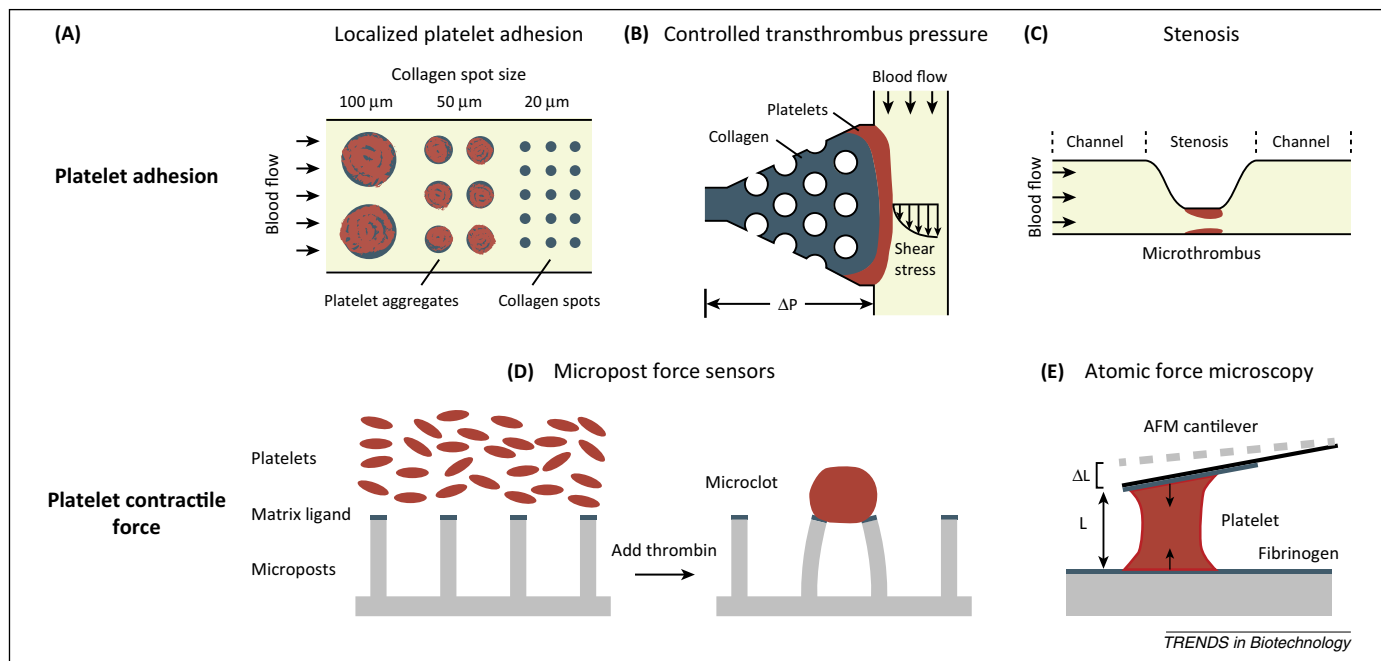


Figure 3. Microengineered devices for measurement of platelet adhesion and contraction. **(A)** Platelet aggregates on collagen spots of different sizes after perfusion with whole blood. A threshold collagen pattern size of 20 μm was necessary for platelet adhesion [63]. Adapted, with permission, from [63]. **(B)** Microfluidic thrombosis device to independently control transthrombus pressure and wall shear stress. Localized collagen plug surrounding posts defines platelet adhesion site. In addition, its permeability allows control of transthrombus pressure [66]. Adapted, with permission, from [66]. **(C)** A microfluidic device with high-shear stenosed region to induce thrombus formation in whole blood [67]. Adapted, with permission, from [67]. **(D)** Micropost array for measurement of platelet contractile force (PCF). Platelets form microclots and exert contractile forces on the micropost force sensors after adding thrombin [80]. Adapted, with permission, from [80]. **(E)** Atomic force microscopy (AFM) for measuring the PCF of single platelets. As a single platelet contracts, its length shortens, causing the AFM cantilever to deflect [83]. Adapted, with permission, from [83].

coagulation, a complex and highly regulated process [60]. Platelet adhesion and contraction are two important functional phenotypes involved in coagulation that have been assessed using newly developed microengineered tools.

Platelet adhesion

Platelet adhesion is the first step in clot formation and is mediated by various plasma and extracellular matrix (ECM) proteins [e.g., von Willebrand factor (VWF), fibrinogen, collagen] and mechanical cues such as the shear force of the blood flow. Failure of platelet adhesion is considered a marker of various coagulation disorders, including von Willebrand disease (vWD), hemophilia A and B, and afibrinogenemia [60]. To reconstruct the process of platelet adhesion during hemostasis, collagen stripes and dots were deposited in microfluidic channels using microfluidic patterning and microcontact printing (μCP) to mimic a wound formed *in vivo* (Figure 3A) [61–63]. The latest version of the device incorporated a parallel-channel design to generate a broad range of shear rates (50–920/s) on the same chip to investigate the effect of shear stress on platelet adhesion and clot formation, with results suggesting a threshold ECM pattern size of 20 μm required for platelet adhesion and faster platelet clotting under higher shear stress conditions [63]. This threshold ECM pattern size for clot formation was also observed in another study using tissue factor (TF) patches of predefined sizes coated on lipid bilayers [64,65]. Another important factor regulating hemostasis is the transthrombus pressure gradient that drives bleeding. This parameter was specifically examined in a microfluidic device that could independently

control shear rate and transthrombus pressure by incorporating multiple fluid/pressure inlets and outlets on a single microfluidic chip (Figure 3B) [66].

In another study targeting thrombosis, a stenosis was included in a microfluidic channel to assess the time needed for a clot to form and completely block the stenosis (i.e., the occlusion time) (Figure 3C) [67]. Real-time blood clot formation was monitored by measuring light transmission through the thrombus: as the thrombus grew, light transmission increased. By integrating multiple channels on the same device, the authors varied flow rates from physiological to pathological conditions (500–13 000/s) and observed that occlusion occurred only at shear rates above 4000/s [67]. Similarly, a microfluidic device containing microscale constrictions was constructed to mimic a stenosis formed in an arteriole [68,69]. Combining this *in vitro* microfluidic system with intravital microscopy, it was demonstrated that hydrodynamics could play a pivotal role in the formation of thrombus at the stenosis.

In addition to shear rate, pressure, and ECM pattern size, microfluidic channels were also utilized to study the effect of agonists/antagonists on platelet adhesion. Microchannels comprising NO-releasing polymers were fabricated to independently tune NO concentration and shear rate [70]. These assays revealed that platelet adhesion and aggregation diminished when NO flux exceeded a certain threshold and completely disappeared if NO flux became too high.

Platelet contraction

In the final step of blood coagulation, the platelet–fibrin clot retracts, resulting in decreased fluid drag [71] and

Review

stiffening of blood clots [72,73]. Blood clot retraction is mediated by actomyosin-based contraction of actin microfilaments in platelets, giving rise to platelet contractile force (PCF) [74]. PCF plays an essential role in coagulation and can serve as a functional marker for platelet dysfunction [75,76]. Various conventional methods (e.g., platelet clot strip [77], clot retractometry [78]) have been developed to measure PCF. However, these techniques are designed for bulk studies and therefore cannot replicate microscale platelet–fibrin interactions and the delicate dynamics of blood clot formation.

Since the concept of PCF is similar to that of the cell traction force exerted by adherent mammalian cells on the ECM, well-established methods for cell traction force measurements have been adapted to assess PCF. For example, traction force microscopy was employed to study the dynamic evolution of PCF during platelet activation, where microbeads were incorporated into the surface of a compliant polymer substrate and platelets were allowed to adhere and exert PCF on the substrate [79]. When the platelets started contracting, displacements of beads were observed and recorded to deduce the force field. Another popular cell traction force measurement tool termed a micropost force sensors was also utilized to measure PCF [80]. Platelets were seeded on top of PDMS microposts pre-coated with fibrinogen or fibronectin to facilitate platelet adhesion. Once platelets were activated by addition of thrombin, deflections of the microposts were observed and recorded to calculate PCF based on the Euler–Bernoulli beam theory (Figure 3D). Variations of this method have been developed to study the effects of glycoprotein Ib and VWF [81], as well as shear force [82], on platelet contraction. In another recent study, custom-built side-view atomic force microscopy (AFM) was used to measure the PCF generated by single platelets bridging the AFM cantilever and a substrate (Figure 3E) [83].

The microengineered tools discussed above for PCF measurements have significantly improved measurement accuracy and sensitivity to unprecedented levels. However, these tools were designed primarily for mechanistic studies of PCF and thus are complicated and suboptimal for direct clinical applications. Automated microengineered tools that are convenient to use for measuring PCF remains to be developed to identify disorders in hemostasis and thrombosis.

Concluding remarks and future perspectives

It is clear that microengineered tools have already made a positive impact on transforming the functional analysis and phenotyping of blood cells. First, microengineered tools consume smaller amounts of blood samples and assay chemicals, making them highly desirable for applications where such resources are limited or costly. Prominent examples include microfluidic immunoassays for pediatric and neonatal patients [47] and platelet functional assays for high-throughput screening (HTS) of antiplatelet drugs [84]. Second, microengineered tools allow precise control and manipulation of blood cells and their microenvironment at a scale comparable to that of single cells and microcapillaries. This enables accurate and sensitive functional analysis of blood cells, such as RBC deformation

and ATP release, WBC deformability, and platelet adhesion and contraction, to unprecedented levels. Finally, microengineered tools bring about exciting opportunities for assay automation by integrated device designs, paving the way for assay standardization and point-of-care applications.

With an increasing number of studies utilizing microengineered tools to reveal fundamental blood cell physiology and the mechanisms of blood-related diseases, most current microdevices are designed for a single type of blood cell only. In reality, each blood cell resides in a complex environment where multiple types of cell coexist and influence each other. To construct more reliable *in vitro* models, a promising approach is organ-on-a-chip devices that can be adapted to construct blood vessel mimics and incorporate multiple blood cell types [85]. Such organ-on-a-chip devices are promising platforms to study endothelium–blood cell and RBC–WBC–platelet interactions. Regarding practical applications such as rapid diagnosis of malaria and HIV/AIDS, microengineered blood cell analysis tools need to be further simplified and automated [86]. Particularly, integration with on-chip blood sample preparation will be required for a much higher degree of device automation.

The field of microengineering is evolving quickly to address the challenges ahead. We believe that future microengineered tools will continue to offer new functionalities, revealing novel insights into blood cell physiology and providing exciting opportunities for advanced clinical diagnosis using minimal blood samples.

Acknowledgments

The authors acknowledge financial support from the National Science Foundation (ECCS 1231826 and CBET 1263889), the National Institutes of Health (1R01HL119542), the American Heart Association (13PRE16510018), the UM-SJTU Collaboration on Biomedical Technologies, the UM Comprehensive Cancer Center Prostate SPOR Pilot Project, the Michigan Institute for Clinical and Health Research (MICH) Pilot Program (UL1RR024986), the Michigan Center for Integrative Research in Critical Care (M-CIRCC), and the Department of Mechanical Engineering at the University of Michigan, Ann Arbor. They apologize to all colleagues in the field whose work they were unable to discuss because of space constraints.

References

- Willmot, M. *et al.* (2004) High blood pressure in acute stroke and subsequent outcome: a systematic review. *Hypertension* 43, 18–24
- Ferrara, G. *et al.* (2006) Use in routine clinical practice of two commercial blood tests for diagnosis of infection with *Mycobacterium tuberculosis*: a prospective study. *Lancet* 367, 1328–1334
- Cristofanilli, M. *et al.* (2004) Circulating tumor cells, disease progression, and survival in metastatic breast cancer. *N. Engl. J. Med.* 351, 781–791
- Piot, P. and Quinn, T.C. (2013) Response to the AIDS pandemic – a global health model. *N. Engl. J. Med.* 368, 2210–2218
- Chien, S. (1987) Red cell deformability and its relevance to blood flow. *Annu. Rev. Physiol.* 49, 177–192
- Bhorade, S.M. *et al.* (2008) Cylex ImmuKnow assay levels are lower in lung transplant recipients with infection. *J. Heart Lung Transplant.* 27, 990–994
- Favaloro, E.J. (2008) Clinical utility of the PFA-100. *Semin. Thromb. Hemost.* 34, 709–733
- Yager, P. *et al.* (2006) Microfluidic diagnostic technologies for global public health. *Nature* 442, 412–418
- Chin, C.D. *et al.* (2007) Lab-on-a-chip devices for global health: past studies and future opportunities. *Lab Chip* 7, 41–57

- 10 Sackmann, E.K. *et al.* (2014) The present and future role of microfluidics in biomedical research. *Nature* 507, 181–189
- 11 Folch, A. and Toner, M. (2000) Microengineering of cellular interactions. *Annu. Rev. Biomed. Eng.* 2, 227–256
- 12 Chen, C.S. *et al.* (2005) Microengineering the environment of mammalian cells in culture. *MRS Bull.* 30, 194–201
- 13 El-Ali, J. *et al.* (2006) Cells on chips. *Nature* 442, 403–411
- 14 Cranston, H.A. *et al.* (1984) *Plasmodium falciparum* maturation abolishes physiologic red cell deformability. *Science* 223, 400–403
- 15 Barabino, G.A. *et al.* (2010) Sickle cell biomechanics. *Annu. Rev. Biomed. Eng.* 12, 345–367
- 16 Sprague, R.S. *et al.* (2001) Impaired release of ATP from red blood cells of humans with primary pulmonary hypertension. *Exp. Biol. Med.* 226, 434–439
- 17 Reid, H. *et al.* (1976) A simple method for measuring erythrocyte deformability. *J. Clin. Pathol.* 29, 855–858
- 18 Carlo, D.D. and Lee, L.P. (2006) Dynamic single-cell analysis for quantitative biology. *Anal. Chem.* 78, 7918–7925
- 19 Hochmuth, R.M. (2000) Micropipette aspiration of living cells. *J. Biomech.* 33, 15–22
- 20 Groner, W. *et al.* (1980) New optical technique for measuring erythrocyte deformability with the ektacytometer. *Clin. Chem.* 26, 1435–1442
- 21 Shevkopyas, S.S. *et al.* (2006) Direct measurement of the impact of impaired erythrocyte deformability on microvascular network perfusion in a microfluidic device. *Lab Chip* 6, 914–920
- 22 Bow, H. *et al.* (2011) A microfabricated deformability-based flow cytometer with application to malaria. *Lab Chip* 11, 1065–1073
- 23 Huang, S. *et al.* (2013) Dynamic deformability of *Plasmodium falciparum*-infected erythrocytes exposed to artesunate *in vitro*. *Integr. Biol. (Camb.)* 5, 414–422
- 24 Zheng, Y. *et al.* (2013) Electrical measurement of red blood cell deformability on a microfluidic device. *Lab Chip* 13, 3275–3283
- 25 Cha, S. *et al.* (2012) Cell stretching measurement utilizing viscoelastic particle focusing. *Anal. Chem.* 84, 10471–10477
- 26 Sprague, R.S. *et al.* (1996) ATP: the red blood cell link to NO and local control of the pulmonary circulation. *Am. J. Physiol. Heart Circ. Physiol.* 271, H2717–H2722
- 27 Sprague, R.S. *et al.* (1998) Deformation-induced ATP release from red blood cells requires CFTR activity. *Am. J. Physiol. Heart Circ. Physiol.* 275, H1726–H1732
- 28 Moehlenbrock, M.J. *et al.* (2006) Use of microchip-based hydrodynamic focusing to measure the deformation-induced release of ATP from erythrocytes. *Analyst* 131, 930–937
- 29 Wan, J. *et al.* (2008) Dynamics of shear-induced ATP release from red blood cells. *Proc. Natl. Acad. Sci. U.S.A.* 105, 16432–16437
- 30 Flynn, J.L. *et al.* (1993) An essential role for interferon gamma in resistance to *Mycobacterium tuberculosis* infection. *J. Exp. Med.* 178, 2249–2254
- 31 Dong, C. *et al.* (1999) Mechanics of leukocyte deformation and adhesion to endothelium in shear flow. *Ann. Biomed. Eng.* 27, 298–312
- 32 Chen, W. *et al.* (2013) Emerging microfluidic tools for functional cellular immunophenotyping: a new potential paradigm for immune status characterization. *Front. Oncol.* 3, 98
- 33 Herrmann, M. *et al.* (2007) Microfluidic ELISA on non-passivated PDMS chip using magnetic bead transfer inside dual networks of channels. *Lab Chip* 7, 1546–1552
- 34 Eteshola, E. and Leckband, D. (2001) Development and characterization of an ELISA assay in PDMS microfluidic channels. *Sens. Actuators B* 72, 129–133
- 35 Herrmann, M. *et al.* (2008) Quantification of low-picomolar concentrations of TNF- α in serum using the dual-network microfluidic ELISA platform. *Anal. Chem.* 80, 5160–5167
- 36 Zhu, H. *et al.* (2008) A microdevice for multiplexed detection of T-cell-secreted cytokines. *Lab Chip* 8, 2197–2205
- 37 Stybayeva, G. *et al.* (2010) Lensfree holographic imaging of antibody microarrays for high-throughput detection of leukocyte numbers and function. *Anal. Chem.* 82, 3736–3744
- 38 Fritzsche, F.S. *et al.* (2012) Single-cell analysis in biotechnology, systems biology, and biocatalysis. *Annu. Rev. Chem. Biomol. Eng.* 3, 129–155
- 39 Wang, D. and Bodovitz, S. (2010) Single cell analysis: the new frontier in 'omics'. *Trends Biotechnol.* 28, 281–290
- 40 Zhu, H. *et al.* (2009) Detecting cytokine release from single T-cells. *Anal. Chem.* 81, 8150–8156
- 41 Love, J.C. *et al.* (2006) A microengraving method for rapid selection of single cells producing antigen-specific antibodies. *Nat. Biotechnol.* 24, 703–707
- 42 Han, Q. *et al.* (2012) Polyfunctional responses by human T cells result from sequential release of cytokines. *Proc. Natl. Acad. Sci. U.S.A.* 109, 1607–1612
- 43 Varadarajan, N. *et al.* (2012) Rapid, efficient functional characterization and recovery of HIV-specific human CD8⁺ T cells using microengraving. *Proc. Natl. Acad. Sci. U.S.A.* 109, 3885–3890
- 44 Fan, R. *et al.* (2008) Integrated barcode chips for rapid, multiplexed analysis of proteins in microliter quantities of blood. *Nat. Biotechnol.* 26, 1373–1378
- 45 Lu, Y. *et al.* (2013) High-throughput secretomic analysis of single cells to assess functional cellular heterogeneity. *Anal. Chem.* 85, 2548–2556
- 46 Beaudet, L. *et al.* (2008) AlphaLISA immunoassays: the no-wash alternative to ELISAs for research and drug discovery. *Nat. Methods* 5, an8–an9
- 47 Huang, N.T. *et al.* (2012) An integrated microfluidic platform for *in situ* cellular cytokine secretion immunophenotyping. *Lab Chip* 12, 4093–4101
- 48 Chen, W. *et al.* (2013) Surface-micromachined microfiltration membranes for efficient isolation and functional immunophenotyping of subpopulations of immune cells. *Adv. Healthc. Mater.* 2, 965–975
- 49 Eyer, K. *et al.* (2013) Implementing enzyme-linked immunosorbent assays on a microfluidic chip to quantify intracellular molecules in single cells. *Anal. Chem.* 85, 3280–3287
- 50 Stern, E. *et al.* (2007) Label-free immunodetection with CMOS-compatible semiconducting nanowires. *Nature* 445, 519–522
- 51 Oh, B-R. *et al.* (2014) Integrated nanoplasmonic sensing for cellular functional immunoanalysis using human blood. *ACS Nano* 8, 2667–2676
- 52 Stern, E. *et al.* (2009) Label-free biomarker detection from whole blood. *Nat. Nanotechnol.* 5, 138–142
- 53 Li, X. *et al.* (2014) Continuous-flow microfluidic blood cell sorting for unprocessed whole blood using surface-micromachined microfiltration membranes. *Lab Chip* 14, 2565–2575
- 54 Drost, E.M. *et al.* (1999) Increased rigidity and priming of polymorphonuclear leukocytes in sepsis. *Am. J. Respir. Crit. Care Med.* 159, 1696–1702
- 55 Pécsvarády, Z. *et al.* (1994) Decreased polymorphonuclear leukocyte deformability in NIDDM. *Diabetes Care* 17, 57–63
- 56 Guo, Q. *et al.* (2012) Microfluidic micropipette aspiration for measuring the deformability of single cells. *Lab Chip* 12, 2687–2695
- 57 Di Carlo, D. (2009) Inertial microfluidics. *Lab Chip* 9, 3038–3046
- 58 Gossett, D.R. *et al.* (2012) Hydrodynamic stretching of single cells for large population mechanical phenotyping. *Proc. Natl. Acad. Sci. U.S.A.* 109, 7630–7635
- 59 George, J.N. (2000) Platelets. *Lancet* 355, 1531–1539
- 60 Harrison, P. (2005) Platelet function analysis. *Blood Rev.* 19, 111–123
- 61 Colace, T. *et al.* (2011) Analysis of morphology of platelet aggregates formed on collagen under laminar blood flow. *Ann. Biomed. Eng.* 39, 922–929
- 62 Neeves, K.B. *et al.* (2008) Microfluidic focal thrombosis model for measuring murine platelet deposition and stability: PAR4 signaling enhances shear-resistance of platelet aggregates. *J. Thromb. Haemost.* 6, 2193–2201
- 63 Hansen, R.R. *et al.* (2013) High content evaluation of shear dependent platelet function in a microfluidic flow assay. *Ann. Biomed. Eng.* 41, 250–262
- 64 Kastrop, C.J. *et al.* (2007) Characterization of the threshold response of initiation of blood clotting to stimulus patch size. *Biophys. J.* 93, 2969–2977
- 65 Kastrop, C.J. *et al.* (2006) Modular chemical mechanism predicts spatiotemporal dynamics of initiation in the complex network of hemostasis. *Proc. Natl. Acad. Sci. U.S.A.* 103, 15747–15752
- 66 Muthard, R.W. and Diamond, S.L. (2013) Side view thrombosis microfluidic device with controllable wall shear rate and transthorbus pressure gradient. *Lab Chip* 13, 1883–1891
- 67 Li, M. *et al.* (2012) Microfluidic system for simultaneous optical measurement of platelet aggregation at multiple shear rates in whole blood. *Lab Chip* 12, 1355–1362

- 68 Nesbitt, W.S. *et al.* (2009) A shear gradient-dependent platelet aggregation mechanism drives thrombus formation. *Nat. Med.* 15, 665–673
- 69 Tovar-Lopez, F.J. *et al.* (2010) A microfluidics device to monitor platelet aggregation dynamics in response to strain rate micro-gradients in flowing blood. *Lab Chip* 10, 291–302
- 70 Sylman, J.L. *et al.* (2013) Transport limitations of nitric oxide inhibition of platelet aggregation under flow. *Ann. Biomed. Eng.* 41, 2193–2205
- 71 Basmadjian, D. (1984) The hemodynamic forces acting on thrombi, from incipient attachment of single cells to maturity and embolization. *J. Biomech.* 17, 287–298
- 72 Jen, C.J. and McIntire, L.V. (1982) The structural properties and contractile force of a clot. *Cell Motil.* 2, 445–455
- 73 Storm, C. *et al.* (2005) Nonlinear elasticity in biological gels. *Nature* 435, 191–194
- 74 Geiger, B. *et al.* (2001) Transmembrane crosstalk between the extracellular matrix and the cytoskeleton. *Nat. Rev. Mol. Cell Biol.* 2, 793–805
- 75 Collet, J. *et al.* (2006) Altered fibrin architecture is associated with hypofibrinolysis and premature coronary atherothrombosis. *Arterioscler. Thromb. Vasc. Biol.* 26, 2567–2573
- 76 Hvas, A.M. *et al.* (2007) Tranexamic acid combined with recombinant factor VIII increases clot resistance to accelerated fibrinolysis in severe hemophilia A. *J. Thromb. Haemost.* 5, 2408–2414
- 77 Cohen, I. and de Vries, A. (1973) Platelet contractile regulation in an isometric system. *Nature* 246, 36–37
- 78 Carr, M.E., Jr (2003) Development of platelet contractile force as a research and clinical measure of platelet function. *Cell Biochem. Biophys.* 38, 55–78
- 79 Henriques, S.S. *et al.* (2012) Force field evolution during human blood platelet activation. *J. Cell Sci.* 125, 3914–3920
- 80 Liang, X.M. *et al.* (2010) Platelet retraction force measurements using flexible post force sensors. *Lab Chip* 10, 991–998
- 81 Feghhi, S. *et al.* (2013) E-beam nanopost arrays reveal that glycoprotein Ib–IV–X complex and von Willebrand factor interactions transmit platelet cytoskeletal forces. In *ASME 2013 Summer Bioengineering Conference*. American Society of Mechanical Engineers, pp. V01BT50A004
- 82 Ting, L.H. *et al.* (2013) Platelet retraction forces induced under high shear gradient activation. In *ASME 2013 Summer Bioengineering Conference*. American Society of Mechanical Engineers, pp. V01BT49A003
- 83 Lam, W.A. *et al.* (2010) Mechanics and contraction dynamics of single platelets and implications for clot stiffening. *Nat. Mater.* 10, 61–66
- 84 Colace, T.V. *et al.* (2013) Microfluidics and coagulation biology. *Annu. Rev. Biomed. Eng.* 15, 283–303
- 85 Huh, D. *et al.* (2012) Microengineered physiological biomimicry: organs-on-chips. *Lab Chip* 12, 2156–2164
- 86 Chin, C.D. *et al.* (2011) Microfluidics-based diagnostics of infectious diseases in the developing world. *Nat. Med.* 17, 1015–1019
- 87 Dudani, J.S. *et al.* (2013) Pinched-flow hydrodynamic stretching of single-cells. *Lab Chip* 13, 3728–3734
- 88 Shelby, J.P. *et al.* (2003) A microfluidic model for single-cell capillary obstruction by *Plasmodium falciparum*-infected erythrocytes. *Proc. Natl. Acad. Sci. U.S.A.* 100, 14618–14622
- 89 Di Carlo, D. *et al.* (2006) Dynamic single cell culture array. *Lab Chip* 6, 1445–1449
- 90 Bernard, A. *et al.* (2000) Microcontact printing of proteins. *Adv. Mater.* 12, 1067–1070
- 91 Kane, R.S. *et al.* (1999) Patterning proteins and cells using soft lithography. *Biomaterials* 20, 2363–2376